

Chapter 10

Fragility Functions of Highway and Railway Infrastructure

Sotiris Argyroudis and Amir M. Kaynia

Abstract The experience of past earthquakes has revealed that highway and railway elements are quite vulnerable to earthquake shaking and induced phenomena such as soil liquefaction or landslide; damages to these elements can seriously affect the transportation of products and people in both short-term (emergency actions) and long-term period. The objective of this chapter is to propose appropriate fragility functions for roadway and railway components other than bridges that are presented separately in Chap. 9. To this end, the main typological features are summarized and a short review of earthquake damages together with damage states definitions are provided for these elements. Fragility curves from literature are collected and reviewed. In some cases these functions are modified and adapted, while in other cases new fragility curves are developed. A general procedure for the derivation of analytical fragility curves that was followed in SYNER-G is described. This approach takes into account the effect of structure geometry, ground motion characteristics, soil conditions and associated uncertainties. New fragility curves are presented for tunnels in soil, embankments, cuttings and bridge abutments based on numerical analyses due to ground shaking. Finally, the proposed fragility functions are summarized and a general scheme to identify the functionality of roadway and railway elements due to different damage levels is outlined.

S. Argyroudis (✉)

Department of Civil Engineering, Aristotle University of Thessaloniki,
54124 Thessaloniki, Greece
e-mail: sarg@civil.auth.gr

A.M. Kaynia

Norwegian Geotechnical Institute (NGI), Ullevål Stadion, N-0806,
P.O. Box. 3930 Oslo, Norway

Department of Structural Engineering, Norwegian University of Science
and Technology (NTNU), 7491 Trondheim, Norway
e-mail: Amir.M.Kaynia@ngi.no

10.1 Introduction

Roadway and railway systems are complex networks of various components like bridges, roads, tunnels, embankments, retaining walls, slopes, tracks and building facilities. Past earthquakes indicate that some of these elements are quite vulnerable, and in addition, involve lengthy repair time or rerouting difficulties. For example, the disruption to the road network can strongly affect the emergency efforts immediately after the earthquake and the rebuilding and other business activities in the following period. Typical paradigms of damage to highway and railway structures can be found in recent earthquakes such as the 2011 Christchurch, New Zealand; 2010 Chile; 2009 L'Aquila, Italy; 2007 Niigata-Chuetsu Oki and 2004 Niigata-ken Chuetsu, Japan and others. In these events the damages due to geotechnical hazards were particularly important.

The complexity of elements at risk, their construction variability, and until recently, the lack of well-documented damage and loss data from strong earthquakes have made the vulnerability assessment of each component or the network as a whole, quite a complicated problem. Consideration of the spatial extension of roadway/railway networks, the interactions with other systems and the inherent uncertainties in seismic hazard and vulnerability estimates, have made the risk assessment of transportation networks a complex and challenging issue.

In the following sections, the main typological features, damage classification and definitions are given for the roadway and railway elements that considered in the SYNER-G taxonomy. A brief review of available fragility curves and their evaluation methods are presented. The existing fragility curves are limited and generally inadequate, especially for the case of induced deformations by liquefaction, lateral spreading, landslide and fault rupture. The derivation of new analytical fragility curves due to seismic shaking is described for specific components and the parameters of the proposed fragility functions are presented. In case of ground failure, preliminary fragility curves are proposed based on expert judgment, while further research is needed on this topic.

10.2 Identification of Main Typologies

Most of the roadway and railway elements are categorized as earth structures; therefore, a main typological feature is the ground type, which characterizes either a construction or its foundation and surrounding material. Different soil classification systems are available based on various soil properties. A widely used scheme is the one provided by Eurocode 8 (2004), which is based on the soil's average shear wave velocity on the top 30 m, V_{s30} .

In case of roadways, the main element is the road itself, which is passing over bridges, embankments or through tunnels and other civil works. Therefore, the hierarchy of roads according to their functions and capacities is an important

parameter for the description of the typologies of the roadway elements. Different classification schemes exist based on speed limits, number of lanes and other criteria.

In case of railway infrastructure, the key part is the track, which consists of elements such as rails, sleepers and ballast that transfer the static and dynamic loads to the foundation soil. Different classification schemes exist which are based on speed limits, construction materials, usage of track and other parameters.

In addition to the above main attributes, other important typological features are given in the following for each element. It is noted that bridges are presented separately in Chap. 9.

- Tunnels: the basic parameters for the description of the typology are the construction method (bored or mined, cut-and-cover, immersed), the shape (circular, rectangular, horseshoe, etc.), the depth (surface, shallow, deep), the geological conditions (rock, alluvial), and supporting system (concrete, masonry, steel, etc.).
- Embankments, cuts and slopes: the main typological features are the geometrical parameters of the construction (i.e. slope angle, height).
- Road pavements: the basic parameter is the number of traffic lanes which is based on the functional hierarchy of the network.
- Bridge abutments: their typology is related to the structural type of bridge (e.g. stub, partial or full depth, integral abutment); other main typological features are the depth and the soil conditions of foundation and fill material behind the abutment. The depth is dependent on the surrounding topography and abutment geometry, while the backfill material behaviour depends on its compaction level.

The typological features and classification considered in SYNER-G are summarized in Table 10.1.

10.3 Damage Description

Earthquake effects on roadway and railway elements can be grouped into two categories, (1) ground shaking (expressed often in terms of peak ground acceleration, PGA); and (2) ground failure such as liquefaction, fault displacement, and slope instability (expressed in terms of permanent ground deformation, PGD). A brief summary is given below for each element:

- Tunnels: Three types of deformations express the response of underground structures to seismic motions, (1) axial compression and extension, (2) longitudinal bending, and (3) ovaling/racking. Typical damages include (Owen and Scholl 1981; ALA 2001; Corigliano 2007): slope instability leading to tunnel collapse, portal failure, roof or wall collapse, invert uplift spalling, cracking or crushing of the concrete lining, slabbing or spalling of the rock around the opening, bending and buckling of reinforcing bars, pavement cracks, wall deformation, local opening of joints and obstruction of the opening.

Table 10.1 SYNER-G taxonomy for roadway and railway network

Category	Sub-category
Bridges	See Chap. 9
Tunnels	Construction method: bored or mined, cut-and-cover, immersed Shape: circular, rectangular, horseshoe, etc. Depth: surface, shallow, deep Geological conditions: rock/alluvial Supporting system: concrete, masonry, steel, etc.
Embankments (road/track on)	Geometrical parameters of the construction, i.e. slope angle, height Soil conditions Water table
Cuts (road/track in)	Geometrical parameters of the construction, i.e. slope angle, height Soil conditions Water table
Slopes (road/track on or running along)	Geometrical parameters of the construction, i.e. slope angle, height Soil conditions Water table
Bridge abutments	Geometry of the abutment i.e. height, width Soil conditions of foundation Fill material behind the abutment
Road pavements (ground failure)	Number of traffic lanes
Railway tracks (ground failure)	Ballasted, slab tracks

- Embankments: When the foundation bearing capacity is lost due to static and dynamic loading, for example due to soil liquefaction, the embankment may spread laterally and settle at the same time. This could lead to lateral movement of embankment (from a few centimetres to several meters) resulting in opening of cracks in the road pavement or displacement of the railway tracks.
- Cuts and slopes: Earthquake induced landslides and rock falls can cause partial or complete blockage of the road/track as well as the structural damage to the road pavement or railway track. In addition, roads/tracks constructed in cuts and on slopes are subjected to failure or large movements of the slopes on the sides of the road/track.
- Bridge abutments/retaining walls: Approach backfills behind bridge abutments/retaining walls are vulnerable to earthquake-induced differential settlement. Approach-fill settlement has been the most commonly occurring type of highway system damage during recent earthquakes. In addition, pounding of the deck to the abutment can seriously affect the overall response of the bridge (Argyroudis et al. 2013a). This type of damage does not often result in extensive repair costs; however, it may have a serious impact on the functionality of the road network during the emergency period. In case of railway network, where the tolerance to ground deformation is lower, the impairment of functionality is more significant.

Table 10.2 Definition of damage states for roadway and railway elements (embankments, cuts, abutments, slopes, tracks) in SYNER-G

Damage state	Permanent ground deformation (m)					
	Roadway			Railway		
	Min	Max	Mean	Min	Max	Mean
DS1. Minor	0.02	0.08	0.05	0.01	0.05	0.003
DS2. Moderate	0.08	0.22	0.15	0.05	0.10	0.008
DS3. Extensive/complete	0.22	0.58	0.40	0.10	0.30	0.200

- Road pavement: Damage to road pavement can be direct (e.g. fault ruptures, settlement, lateral spreading) or indirect (e.g. collapsed buildings, landslide debris, damage to underlying pipelines).
- Railway track damage in past earthquakes have included displaced ballast, broken ties, pulled apart joints, broken rails, buckled rail, large lateral displacements and loss of vertical support for track over large distances. Signal systems have suffered limited damages in relatively low magnitude earthquakes due to broken batteries, overturned electrical relays and wrapped wires in pole lines. Such damage are often highly disruptive but can be quickly repaired. Moreover, losses might occur in larger earthquakes in terms of more extensive damage such as broken signal masts (Byers 2004).

Different damage criteria have been proposed for the fragility analysis of roadway and railway elements. The number of damage states is variable and is related with the functionality, traffic state, and/or the repair duration. In empirical and expert judgment methods, the extent of damage is described qualitatively (e.g. extent of cracks or settlements). In analytical methods the damage levels are defined based on the range of a specific damage index such as permanent ground deformation, capacity and factor of safety, which is also related to the serviceability level of the network.

The damage states in Table 10.2, in terms of permanent ground deformation (PGD), have been proposed in SYNER-G and have been used for roadway and railway components. In particular, a mean value of PGD was estimated for minor, moderate, and extensive/complete damage based on a range of values (min, max) from a review of the literature. In Table 10.3 and Table 10.4 the damage states for each component are defined and also correlated to the serviceability of the network.

10.4 Review of Existing Fragility Functions

The existing fragility functions are based on empirical, analytical or expert judgment methods. Most of the available fragility curves follow a lognormal cumulative distribution. The number of damage states and the type of intensity measure vary

Table 10.3 Description of damage states for roadway/railway components in SYNER-G

Description	Serviceability
Tunnels	
DS1 Minor cracking and spalling and other minor distress to tunnel liners	Open to traffic, closed or partially closed during inspection, cleaning and possible repair works
DS2 Ranges from major cracking and spalling to rock falls	Closed during repair works for 2–3 days
DS3 Collapse of liner or surrounding soils to the extent that the tunnel is blocked either immediately or within a few days after the main shock	Closed for a long period of time
Metro/urban tunnels in soil	
DS1 Minor cracking and spalling and other minor distress to tunnel lining	Open to traffic, closed or partially closed during inspection and possible repair works
DS2 Major cracking and spalling of tunnel lining	Closed during repair works for 2–3 days
DS3 Extensive damage of liner or surrounding soils to the extent that the tunnel is blocked either immediately or within a few days after the main shock	Closed for a long period of time
Embankments (road/track on)	
DS1 Surface slide of embankment at the top of slope; minor cracks on road surface; minor track displacement	Open, reduced speed
DS2 Deep slide or slump of embankment; medium cracks on road surface and/or settlement; medium track displacement	Partially open during repairs (roadway). Closed during repairs (railway)
DS3 Extensive slump and slide of embankment; extensive cracks on road surface and/or settlement; extensive tracks displacement	Partially open during repair or closed during reconstruction works (roadway). Closed (railway)
Cuts (road/track in)	
DS1 Surface slide; minor cracks on road surface; minor displacement of the tracks	Open, reduced speed
DS2 Deep slide or slump; medium cracks on road surface and/or settlement; medium displacement of the tracks	Partially open during repairs (roadway). Closed during repairs (railway)
DS3 Extensive slump and slide; extensive cracks on road surface and/or settlement; extensive displacement of the tracks	Partially open or closed during repairs/reconstruction (roadway). Closed (railway)

depending on the method and the element at risk. Most common intensity measure types (IMTs) are peak ground acceleration (PGA) when ground shaking is the cause of damage or permanent ground deformation (PGD) in case of ground failure. A brief review of existing fragility functions for roadway and railway elements is given in the following. The corresponding review of methods and IMTs for bridges is provided in Chap. 9.

Table 10.4 Description of damage states for roadway/railway components in SYNER-G (cont.)

Description	Serviceability
Bridge abutments	
DS1 Minor settlement of approach fill (roadway: 2–8 m; railway: 1–5 cm)	Open. Reduced speeds or partially closed during repair
DS2 Moderate settlement of approach fill (roadway: 8–22 cm; railway: 5–10 cm)	Closed or partially closed during repair works (roadway). Closed (railway)
DS3 Extensive settlement of approach fill (roadway: >22 cm; railway: >10 cm)	Closed during repair/reconstruction works
Slopes (road/track on or running along)	
DS1 Surface slide at top of slope; minor cracks on road surface; minor track displacement	Open, reduced speed
DS2 Deep slide or slump; medium cracks on road surface and/or settlement; medium displacement of the track	Partially open or closed during repairs (roadway). Closed during repairs (railway)
DS3 Extensive slump and slide; extensive cracks on road surface; extensive displacement of the track	Closed during repairs/reconstruction
Road pavements	
DS1 Slight cracking/offset of pavement surface	Open. Reduced speeds or partially closed during repair works
DS2 Localized moderate cracking/offset of pavement	Closed during repairs (few days)
DS3 Major cracking/offset of pavement and subsurface soil	Closed during repairs (few days to weeks)
Tracks	
DS1 Minor (localized) derailment due to slight differential settlement of embankment or ground offset	Operational after inspection or short repairs
DS2 Considerable derailment due to differential settlement or ground offset	Closed to traffic. Local repairs or replacement of tracks is required
DS3 Major differential settlement of the ground resulting in potential derailment over extended length	Closed to traffic. Replacement of track's segments is required. Duration of closure depends on length of damaged lines

10.4.1 Tunnels

Until recently, the vulnerability assessment of tunnels has mainly been based on expert judgment (ATC13 1985; NIBS 2004) or empirical fragility curves (ALA 2001; Corigliano 2007) derived from actual damage in past earthquakes. In the study by Corigliano (2007) all deep tunnels are classified in one category and the proposed fragility curves are given as functions of peak ground velocity (PGV) for none/slight and moderate damage. The HAZUS approach (NIBS 2004) is based on judgment and limited empirical data set by Dowding and Rozen (1978) and Owen and Scholl (1981), providing fragility curves both for ground shaking (PGA) and ground failure (PGD). In ALA approach tunnels are distinguished based on

Table 10.5 Fragility function parameters for tunnels (ALA 2001)

Typology	Damage state	μ (g)	β
Rock tunnels with poor-to-average construction and conditions	Minor/slight	0.35	0.4
	Moderate	0.55	0.4
	Heavy	1.10	0.5
Rock tunnels with good construction and conditions	Minor/slight	0.61	0.4
	Moderate	0.82	0.4
	Heavy	NA	–
Alluvial (soil) and cut and cover tunnels with poor to average construction	Minor/slight	0.30	0.4
	Moderate	0.45	0.4
	Heavy	0.95	0.5
Alluvial (soil) and cut and cover tunnels with good construction	Minor/slight	0.50	0.4
	Moderate	0.70	0.4
	Heavy	NA	–

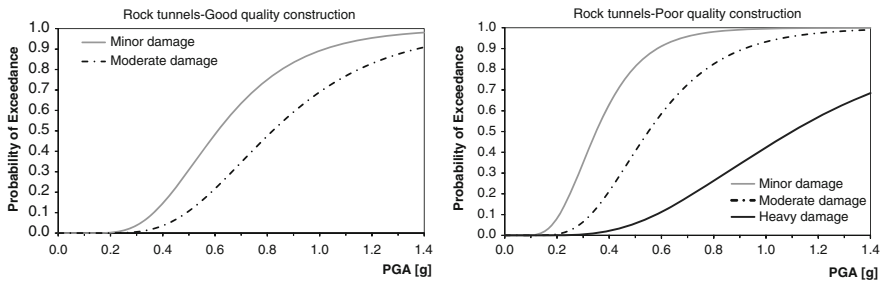


Fig. 10.1 Fragility curves for tunnels in rock (ALA 2001)

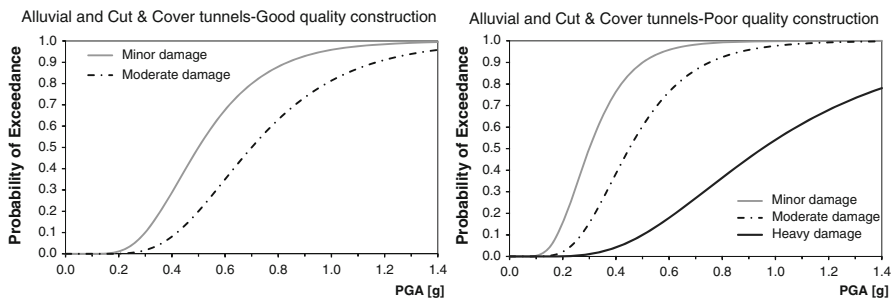


Fig. 10.2 Fragility curves for tunnels in alluvial and cut and cover (ALA 2001)

geology conditions and quality of construction. Fragility curves are given as functions of PGA for three damage states. The parameters of the lognormal distribution in terms of medians (μ) and standard deviations (β) are given in Table 10.5. The fragility curves are illustrated in Figs. 10.1 and 10.2.

A limited number of numerical approaches for the fragility analysis of tunnels are available. Salmon et al. (2003) presented analytical fragility curves for bored and cut and cover tunnels of the BART project as a function of PGA (ground shaking) and PGD (fault offset). These curves are site specific and their use is limited to the BART project. In the framework of LessLoss (2007) project, Argyroudis and Pitilakis (2007) proposed a preliminary set of analytical fragility curves for circular (bored) tunnels due to permanent ground deformation (PGD).

In the SYNER-G project new analytical fragility curves were proposed for shallow/metro tunnels in alluvial soil for different conditions (circular/bored and rectangular/cut and cover) due to ground shaking (see Sect. 10.5.2). In case of permanent ground deformations the generic fragility curves by HAZUS methodology can be applied as a first approximation, however further research is needed on this topic.

10.4.2 Embankments, Cuts and Slopes

Maruyama et al. (2010) proposed empirical curves for expressway embankments based on damage datasets from recent earthquakes in Japan. The fragility functions relate the number of damage incidents per km of expressway to PGV. Lagaros et al. (2009) proposed analytical fragility curves for embankments based on pseudostatic slope stability analyses, through Monte Carlo simulation method and neural network metamodels. The damage states are defined based on factor of safety, while the main purpose of the study is to highlight the computational effort of different approaches. The ATC-13 (1985) approach provided fragility curves for six slope classes, which are defined by the critical acceleration based on expert opinion as a function of earthquake intensity MMI. Finally, an expert judgment approach to determining the physical vulnerability of roads for a given debris flow volume is proposed by Winter et al. (2013). Damage probabilities were assessed based on a detailed questionnaire to experts.

In the framework of SYNER-G, new analytical fragility curves have been developed as functions of PGA, for embankments and cuts of different heights and soil conditions (see Sect. 10.5.4). In case of roads and tracks on slopes new fragility curves were proposed following the approach adopted by Pitilakis et al. (2010). In particular, the threshold PGD values of Table 10.2 were used for the estimation of the corresponding PGA medians based on the model by Bray and Travararou (2007). The slopes were classified through the yield acceleration coefficient k_y (Table 10.6, Figs. 10.3 and 10.4).

10.4.3 Retaining Walls and Approach Fills

The ATC-13 (1985) approach provided damage probability matrices for retaining walls for different levels of MMI based on expert opinion. Salmon et al. (2003)

Table 10.6 Fragility function parameters for roads and tracks on slopes

Typology	Damage state	$k_y = 0.05$		$k_y = 0.1$		$k_y = 0.2$		$k_y = 0.3$	
		μ (g)	β	μ (g)	β	μ (g)	β	μ (g)	β
Road on or running along slope	Minor	0.14	0.40	0.25	0.35	0.45	0.35	0.64	0.30
	Moderate	0.22	0.40	0.40	0.35	0.71	0.35	1.00	0.30
	Extensive/ complete	0.37	0.40	0.64	0.35	1.11	0.35	1.55	0.30
Track on or running along slope	Minor	0.11	0.60	0.20	0.60	0.37	0.60	0.52	0.60
	Moderate	0.17	0.60	0.30	0.60	0.54	0.60	0.78	0.60
	Extensive/ complete	0.26	0.60	0.45	0.60	0.80	0.60	1.13	0.60

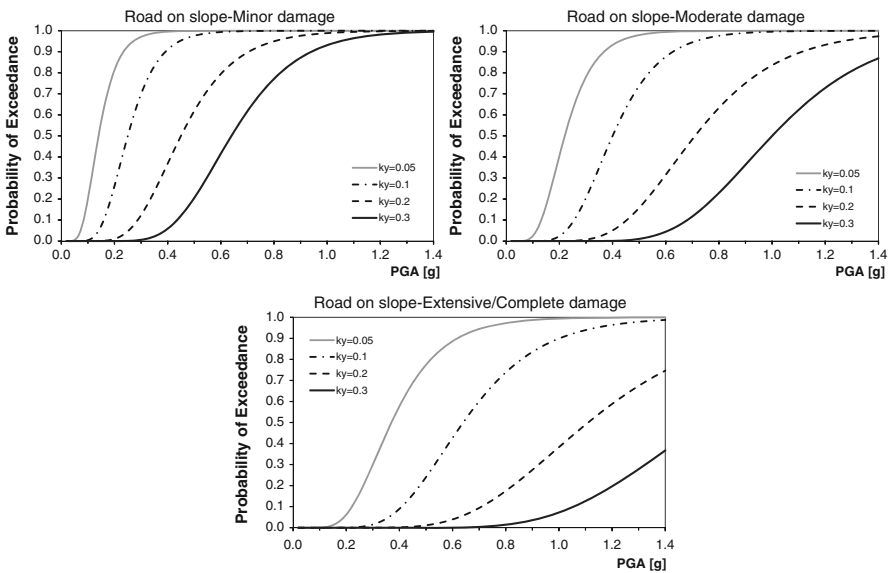


Fig. 10.3 Fragility curves at various damage states and different yield coefficients (k_y) for roads on slope (Kaynia 2013)

reported analytical fragility curves for retaining walls of the BART project as functions of PGA. However, the typological characteristics of the walls are not given; therefore, the fragility functions are considered as project specific. REDARS methodology (Werner et al. 2006) provides threshold values of PGD for different damage levels, related to the repair cost, duration and traffic states of bridge approach fills and road pavements for California highways. They are based on expert judgment and are not given in the form of fragility functions.

In the framework of SYNER-G, new analytical curves for bridge abutments on shallow foundations are proposed as functions of PGA for different soil conditions and abutment heights (see Sect. 10.5.3).

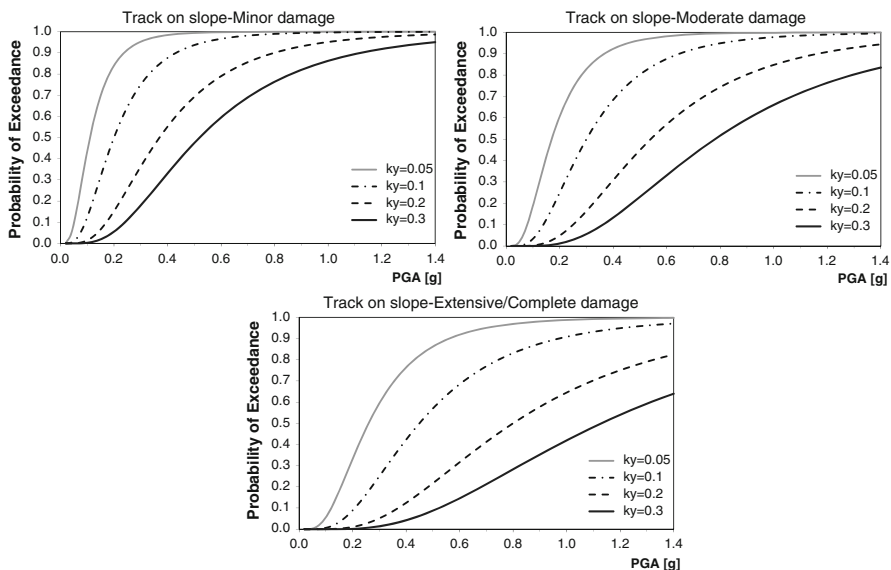


Fig. 10.4 Fragility curves at various damage states and different yield coefficients (k_y) for tracks on slope (Kaynia 2013)

Table 10.7 Fragility function parameters for road pavements

Typology	Damage state	μ (m)	β
2 traffic lanes (Urban roads)	Minor	0.15	0.7
	Moderate	0.30	0.7
	Extensive/complete	0.60	0.7
≥ 4 traffic lanes (Major roads)	Minor	0.30	0.7
	Moderate	0.60	0.7
	Extensive/complete	1.50	0.7

10.4.4 Road Pavements and Railway Tracks

HAZUS methodology (NIBS 2004) includes fragility curves for major and urban roads as functions of PGD (fault offset, liquefaction, landslide) (Table 10.7, Fig. 10.5). These curves have been validated in SYNER-G using observed damage in road pavements during past earthquakes in Greece. The results indicated a good agreement between the estimated and observed damages (Kaynia et al. 2011). The aforementioned functions, which are based on expert judgment, are also suggested for railway tracks in HAZUS methodology. However, the tolerance of railways to damage is lower and therefore these functions are generally considered unsatisfactory. In SYNER-G, new PGD thresholds to different damage states have been proposed for railway tracks. These values are applied for the derivation of fragility

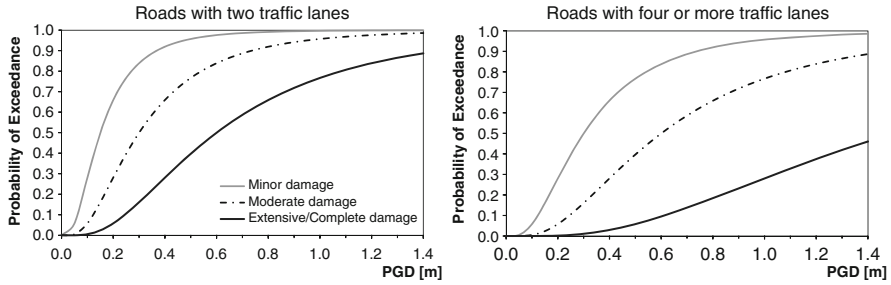


Fig. 10.5 Fragility curves for road pavements subjected to ground failure (NIBS 2004)

Table 10.8 Fragility function parameters for railway tracks

Damage state	μ (m)	β
Minor	0.03	0.70
Moderate	0.08	0.70
Extensive/complete	0.20	0.70

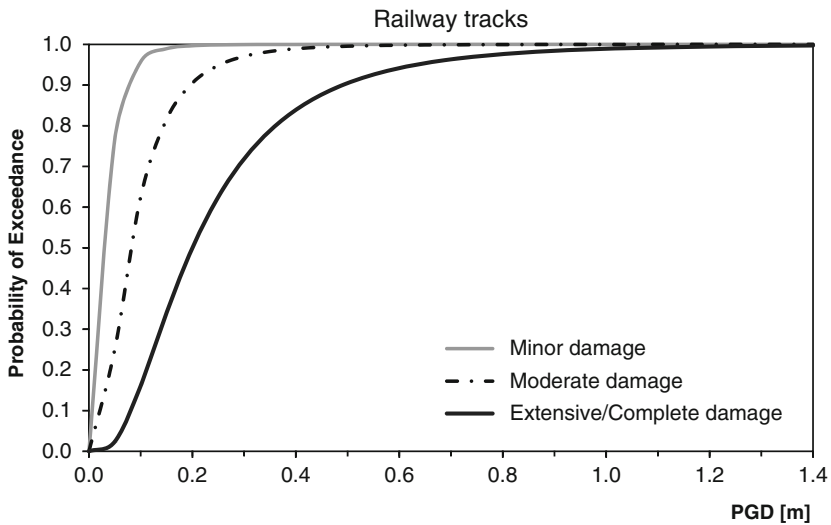


Fig. 10.6 Fragility curves for railway tracks subjected to ground failure (Kaynia 2013)

functions for railway tracks subjected to ground failure (Table 10.8 and Fig. 10.6). As a first approximation, these fragility curves can be applied for road pavements and railway tracks subjected to permanent ground deformations (e.g. by liquefaction, fault crossing, and landslide) independently of their location on embankment, cut, slope or flat ground. However, further investigation is needed on this subject to study the effects of soil and topography conditions as well as the peculiarities of each component.

10.5 New Analytical Fragility Curves for Ground Shaking

The existing fragility curves for roadway and railway components are mainly based on empirical or expert judgment approaches both for ground shaking and ground failure. In many cases they do not cover adequately the typologies, soil conditions and ground motion characteristics. In the framework of SYNER-G, new analytical fragility curves were developed for tunnels in alluvial soil and roadway/railway bridge abutments, embankments and cuts subjected to ground shaking. In the following, a brief description of the general procedure for the derivation of the analytical fragility curves is given. Next, the main modeling issues are described, and finally, the parameters of the new fragility curves are summarized for each component. The response of roadway and railway infrastructures due to earthquake-induced geohazards such as landslides and ground failure needs further research in order to develop adequate fragility curves for all elements.

10.5.1 Key Modeling Issues and Treatment of Uncertainties

The general procedure followed in SYNER-G for the derivation of analytical fragility curves for roadway and railway elements is described by Argyroudis et al. (2013b). The effects of soil conditions and ground motion characteristics on the element's response are taken into account by using different typical soil profiles and seismic input motions. The response of the free field soil profiles is calculated through 1D numerical analysis with increasing ground motion amplitude at the seismic basement ($V_s > 800$ m/s). 2D dynamic or quasi-static analysis is used for the non-linear seismic response of the soil-structure. This approach allows the evaluation of fragility curves considering the distinctive features of the element geometries, the input motion characteristics and the soil properties.

The level of damage is described by a damage index expressing the exceedance of certain limit states (Table 10.2), and the fragility curves are estimated based on the evolution of damage index with increasing earthquake acceleration, considering the associated uncertainties. An example is given in Fig. 10.7 where the different points indicate the results of the analyses in terms of damage index for different levels of earthquake shaking. The solid line is produced based on a regression analysis in which the median threshold value of the intensity measure to cause the i_{th} damage state is estimated based on the definition of damage index (mean values in Table 10.2). The fragility curve is described by a lognormal distribution function which is defined by two parameters, the median threshold value of the earthquake intensity measure type IMT (e.g. PGA) required to cause the i_{th} damage state and the total standard deviation, β_{tot} , which describes the total variability associated with each fragility curve. Three primary sources of uncertainty are usually considered (NIBS 2004), namely the definition of damage states, β_{DS} , the response and

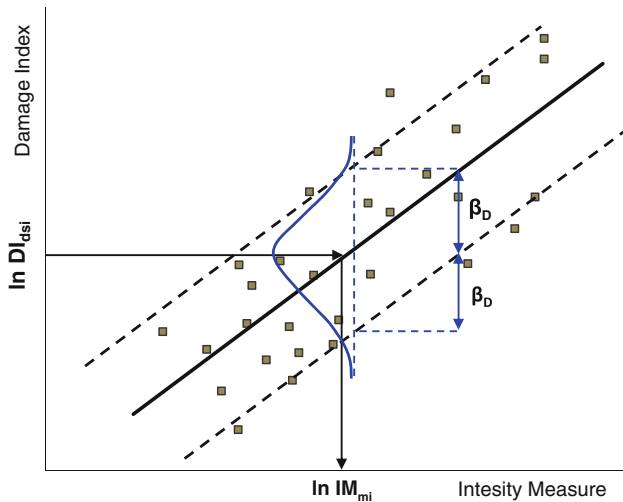


Fig. 10.7 Example of evolution of damage with earthquake intensity measure and definition of threshold median value for the damage state i , and definition of standard deviation (β_D) due to input motion (demand)

resistance (capacity) of the element, β_C , and the earthquake input motion (demand), β_D . The total uncertainty is estimated as the root of the sum of the squares of the component dispersions assuming that they are stochastically independent lognormal-distributed random variables.

In the absence of a more rigorous estimation, the uncertainty parameters can be obtained from the literature (e.g. NIBS 2004). However, the uncertainty associated with seismic demand (β_D), is described by the variability in response due to the variability of ground motion in numerical simulations.

10.5.2 Shallow Tunnels

Numerical fragility curves for shallow metro (urban) tunnels in alluvial deposits were developed by considering structural parameters, local soil conditions and – input ground motion characteristics. In particular, the transverse seismic response of the tunnel due to upward travelling shear waves was evaluated under quasi-static conditions by applying on the tunnel cross-section and the surrounding soil the free field seismic ground deformations, which were calculated independently though 1D equivalent linear analysis. Different tunnel cross-sections, input motions and soil profiles were employed. By defining the damage levels according to the exceedance of strength capacity of the most critical sections of the tunnel, the fragility curves were constructed as functions of the level and the type of seismic excitation. The comparison between the new fragility curves and the existing empirical ones has highlighted the important role of the local soil conditions (Argyroudis and Pitilakis 2012).

Table 10.9 Definition of damage states for tunnel lining

Damage state (DS)	Range of damage index (DI)	Central value of damage index
DS1. Minor/slight	$1.0 < M/M_{Rd} \leq 1.5$	1.25
DS2. Moderate	$1.5 < M/M_{Rd} \leq 2.5$	2.00
DS3. Extensive	$2.5 < M/M_{Rd} \leq 3.5$	3.00
DS4. Collapse	$M/M_{Rd} > 3.5$	–

10.5.2.1 Damage States

The damage states of existing empirical fragility curves are based on a qualitative damage description from past earthquakes. In the present study the damage index (DI) is defined as the ratio between the bending moment demand, M , and the capacity bending moment of the tunnel cross-section, M_{Rd} . This definition is compatible with the use of displacements, according to the equal displacement approximation. Based on previous experience of damages in shallow tunnels and applying engineering judgment, four damage states were considered due to ground shaking. They refer to minor, moderate, extensive and complete damage of the tunnel lining as described in Table 10.9.

10.5.2.2 Model Parameters

Two typical tunnel sections were considered, a circular (bored) tunnel with a 10 m diameter and a rectangular (cut and cover) one-barrel frame with dimensions 16×10 m. The lining of the circular tunnel is composed of 0.50 m thick precast concrete segments, while the rectangular tunnel has 0.9 m thick concrete walls, 1.2 m thick roof slab and 1.4 m thick base slab. The circular and rectangular tunnel was placed at 10 m and 3.5 m depths, respectively. Fourteen ideal soil deposits were considered corresponding to ground types B, C and D of Eurocode 8 (2004), ranged according to the shear wave velocity, V_{s30} , values. Three different soil thicknesses equal to 30, 60 and 120 m were assumed, and typical values of the different soil parameters were selected for each soil layer.

Records on rock sites from different earthquakes were selected such that their average response spectrum matched fairly well the response spectrum of Eurocode 8. These earthquake records were scaled from 0.1 to 0.7 g and used as input motion in 1D ground response analyses. The estimated seismic ground deformations were applied on the boundaries of the soil-tunnel model in order to calculate the induced stresses in the tunnel as a function of PGA and finally to estimate the fragility curves (Argyroudis and Pitilakis 2012).

10.5.2.3 1D and 2D Numerical Analyses

The imposed quasi-static seismic ground displacements were computed using 1D equivalent linear approach with the code EERA (Bardet et al. 2000). The variations

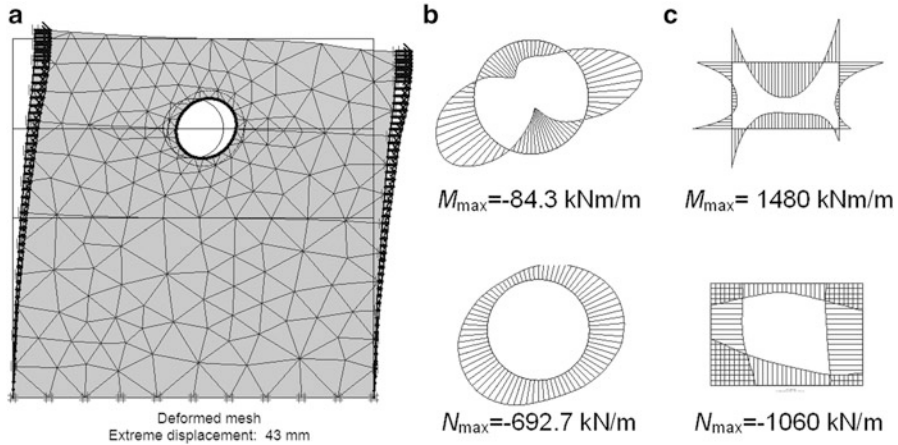


Fig. 10.8 Example of 2D analysis of tunnel: deformed mesh (a), total moment and axial forces of the circular (b) and rectangular (c) tunnel lining (soil profile: type B, depth: 60 m; input motion: Kypseli, 0.3 g)

of shear modulus G/G_0 (where G_0 is the initial shear modulus) and damping ratio with the shear strain level γ were defined according to the available data in the literature as a function of plasticity index and effective stress. The PGA value computed on the surface of each soil profile was selected as the representative IMT in the fragility curves.

A plane strain ground model with the tunnel cross-section was analysed using the finite element code PLAXIS 2D (Plaxis 1998). Prior to the application of the imposed displacement, a set of initial static analyses was performed to properly model the initial static conditions, the excavation of the tunnel and the construction of the lining. The behaviour of the tunnel lining is assumed to be linear elastic, while the soil was characterized by a Mohr-Coulomb yield criterion in all the stages of the analysis. Figure 10.8 shows a representative example of the tunnel response after imposing the shear ground displacements.

10.5.2.4 Derivation of Fragility Curves

For the derivation of fragility curves the general procedure described in Sect. 10.5.1 is followed. In particular, the median PGA value for each damage state is based on the relationship between the computed damage indices versus PGA on the free field and the definitions of damage states given in Table 10.9. A value equal to 0.4 was assigned for the uncertainty associated with the definition of damage states, β_{DS} , following the approach of HAZUS (NIBS 2004) for buildings; the uncertainty due to the capacity, β_C , is assigned equal to 0.3 according to analyses for bored tunnels of BART system (Salmon et al. 2003). The last source of uncertainty, associated with seismic demand, is described by the standard deviation of the damage indices

Table 10.10 Parameters of numerical fragility curves for urban tunnels in different ground types

Typology	Damage state	Ground type B		Ground type C		Ground type D	
		μ (g)	β	μ (g)	β	μ (g)	β
Circular urban tunnels	Minor	1.24	0.55	0.55	0.70	0.47	0.75
	Moderate	1.51	0.55	0.82	0.70	0.66	0.75
	Extensive	1.74	0.55	1.05	0.70	0.83	0.75
Rectangular urban tunnels	Minor	0.75	0.55	0.38	0.55	0.36	0.55
	Moderate	1.28	0.55	0.76	0.55	0.73	0.55
	Extensive	1.73	0.55	1.08	0.55	1.05	0.55

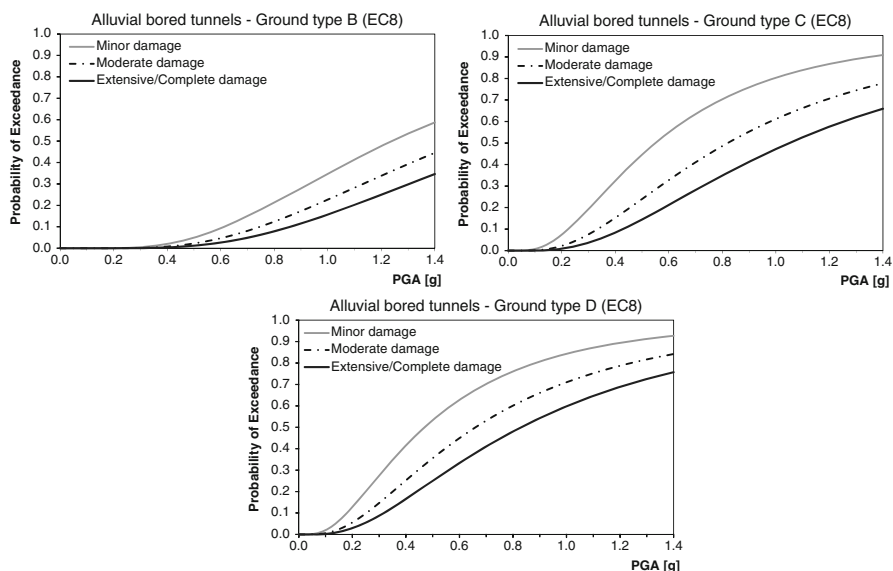


Fig. 10.9 Fragility curves for circular (bored) metro/urban tunnel section

that have been calculated for the different input motions at each level of PGA. The parameters of the lognormal distribution in terms of medians and standard deviations are given in Table 10.10 and the corresponding fragility curves are shown in Figs. 10.9 and 10.10.

10.5.3 Bridge Abutments

New analytical fragility curves for bridge abutment-approach fill system were developed in SYNER-G (Argyroudis et al. 2013b). The response of the abutment was evaluated from dynamic analyses with an increasing level of seismic shaking

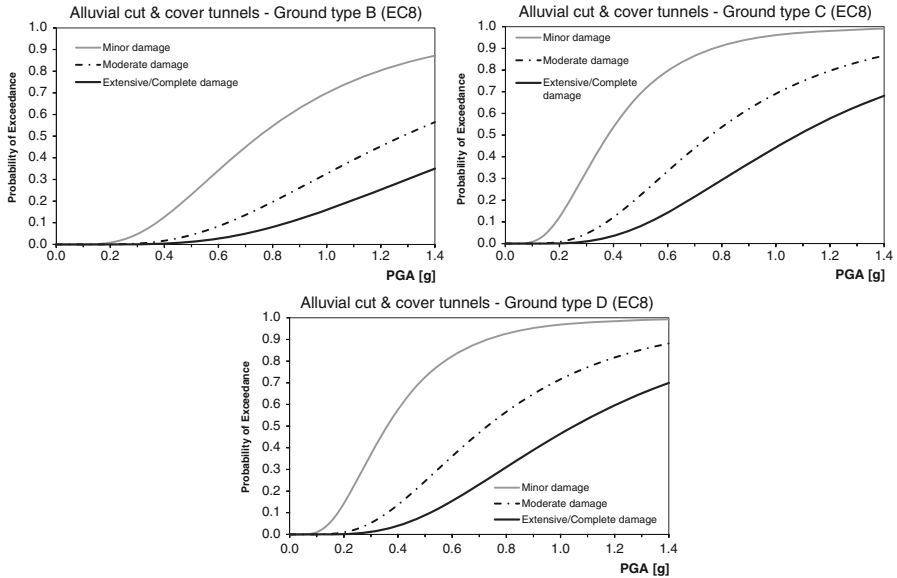


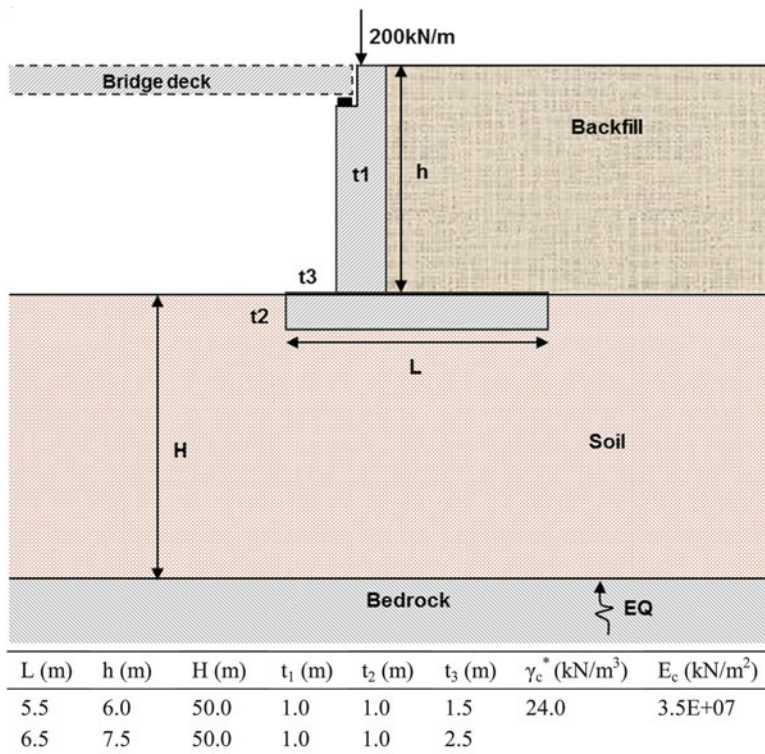
Fig. 10.10 Fragility curves for rectangular (cut and cover) metro/urban tunnel section

following the general procedure briefly described in Sect. 10.5.1. In particular, the soil behaviour was simulated through a 2D fully coupled FE model using an elastoplastic criterion. A calibration procedure was followed in order to account for the dependency of both stiffness and damping on the ground strain level. The effect of soil conditions and ground motion characteristics in the global soil and structure response was taken into account by considering different typical soil profiles and seismic input motions. The performance of the wall, and thus the level of damage, was described by the settlement observed on the backfill.

10.5.3.1 Model Parameters

Representative and simplified bridge abutment geometries with two different heights equal to 6.0 and 7.5 m were modeled as cantilever retaining wall (Fig. 10.11). The bridge deck is supported by the abutment on bearings while its total load is simulated by a vertical load equal to 200 kN.

Five real earthquake records were selected such that their average response spectrum matched fairly well the response spectrum of Eurocode 8 on rock. The earthquake records were from: Kocaeli 1999, Gebze; Hector Mine 1999, Hector; Parnitha 1999, Kypseli; Loma Prieta 1989, Diamond Height; Umbria Marche 1998, Gubbio-Piana. The time histories of these records were scaled from 0.1 to 0.5 g and were applied at the base of the soil model in order to calculate the response of the backfill-abutment due to an increasing level of seismic intensity.



* γ_c: unit weight of concrete

Fig. 10.11 Properties of soil/backfill/abutment under study

Two ideal soil deposits of 50 m, corresponding to ground types C and D in Eurocode 8 were considered. Typical values of the soil parameters were selected for both the soil profile and the backfill. The 1D ground response analyses were performed using 1D equivalent linear approach with the code EERA (Bardet et al. 2000). A calibration procedure was followed in order to account for the dependency of both stiffness and damping on the strain level. Details for the model parameters are given in Argyroudis et al. (2013b).

The numerical simulations were performed using the finite element code PLAXIS 2D (Plaxis 2011). A close-up of the mesh employed in the study is shown in Fig. 10.12. All the analyses were carried out by performing a set of initial static stages to simulate the initial weight, the installation of the abutment and the backfill, followed by the dynamic analyses.

10.5.3.2 Derivation of Fragility Curves

The derivation of the fragility curves from the results of the numerical simulations was similar to that presented in Sect. 10.5.1. The threshold PGD values of Table 10.2

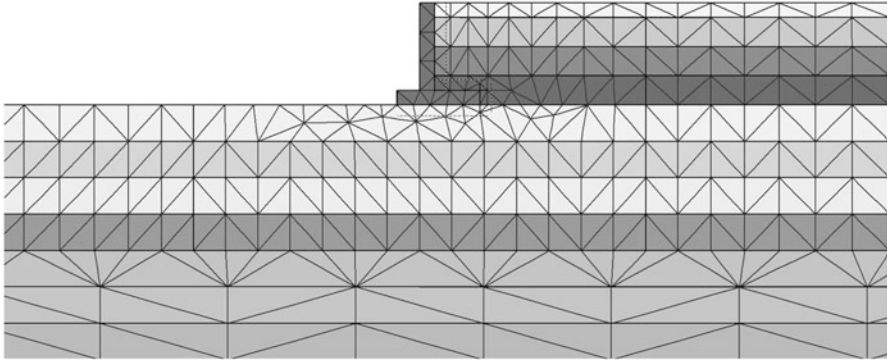


Fig. 10.12 Finite element mesh used in the analyses of bridge abutment

Table 10.11 Parameters of numerical fragility curves for roadway and railway abutments in different ground types

Typology	Damage state	Ground type C				Ground type D			
		h = 6 m		h = 7.5 m		h = 6 m		h = 7.5 m	
		μ (g)	β	μ (g)	β	μ (g)	β	μ (g)	β
Roadway	Minor	0.38	0.70	0.26	0.70	0.20	0.90	0.18	0.90
	Moderate	0.64	0.70	0.52	0.70	0.45	0.90	0.39	0.90
	Extensive/ complete	1.02	0.70	0.97	0.70	0.93	0.90	0.78	0.90
Railway	Minor	0.29	0.70	0.19	0.70	0.14	0.90	0.12	0.90
	Moderate	0.46	0.70	0.34	0.70	0.27	0.90	0.23	0.90
	Extensive/ complete	0.73	0.70	0.63	0.70	0.56	0.90	0.47	0.90

were used for the estimation of median PGA values for each damage state through the corresponding diagrams that describe the evolution of damage with PGA. The parameters of the fragility curves are presented in Table 10.11. The fragility curves for complete damage are derived based on extrapolation of the available computed results. Damage records from a recent earthquake in Japan were used to validate the proposed fragility curves (Argyroudis et al. 2013b) (Figs. 10.13 and 10.14).

10.5.4 Embankments and Cuts

New analytical fragility curves for embankments and cuts were developed in SYNER-G. The response of the system was evaluated based on dynamic analyses with increasing level of seismic intensity following the procedure described in Sect. 10.5.1. Further developments for the seismic performance and fragility assessment of roadway embankments are provided in Argyroudis and Kaynia (2013).

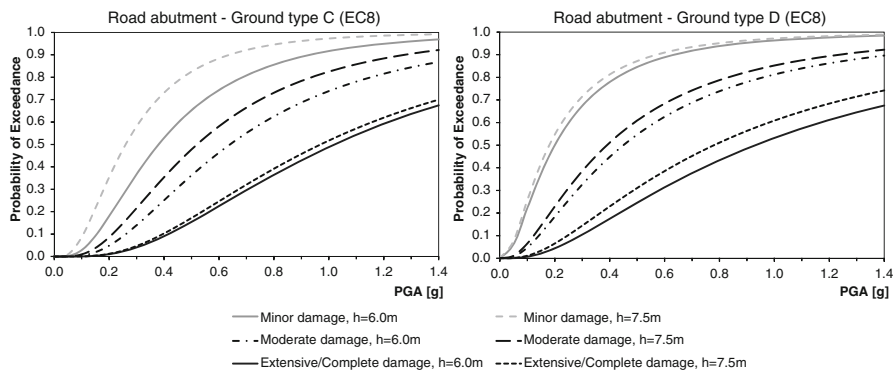


Fig. 10.13 Fragility curves for road abutments, ground type C (left) and D (right)

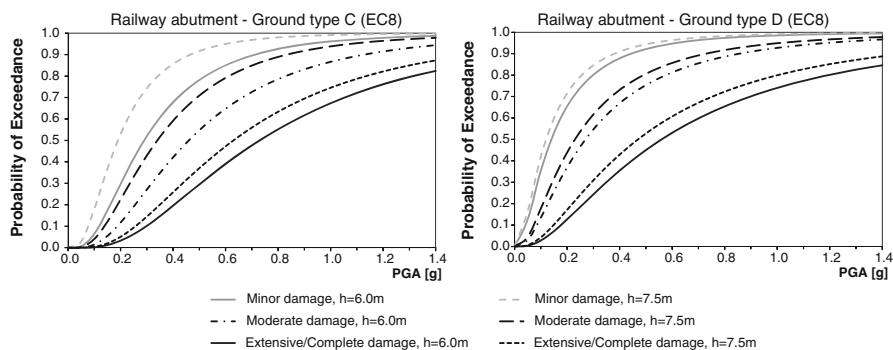


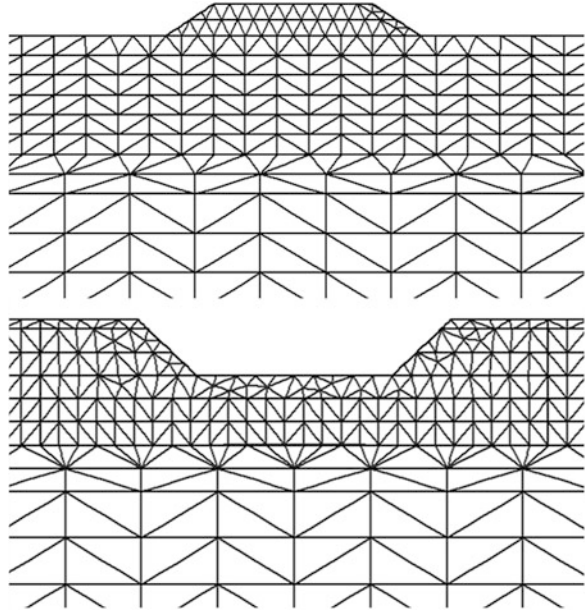
Fig. 10.14 Fragility curves for railway abutments, ground type C (left) and D (right)

10.5.4.1 Model Parameters

Representative geometries are considered with heights equal to 2.0 and 4.0 m for the embankment and 4.0 and 6.0 m for the cut; preliminary analyses indicated that typical engineered cuttings shallower than 4.0 m are practically not vulnerable to earthquake shaking. The top width of the embankment and the bottom width of the cut is 20 m. The same earthquake records used in the analysis of bridge abutments were applied in these analyses. The earthquake time histories were scaled from 0.1 to 0.7 g and the response of embankment/cut is calculated as a function of PGA on the ground surface.

Two ideal soil deposits of 50 m corresponding to ground types C and D with shear wave velocity (V_{s30}) in the range defined by Eurocode 8 were considered

Fig. 10.15 Finite element mesh used in the analyses of embankment (*up*) and cut (*down*)



similar to those used in case of abutments. Typical values of soil properties are selected for the embankment. The numerical simulations are performed with the finite element code PLAXIS 2D (Plaxis 2011). A close-up of the models is shown in Fig. 10.15.

10.5.4.2 Derivation of Fragility Curves

The derivation of fragility curves was based on a diagram of the computed damage indices in terms of average total permanent ground deformation, PGD, on embankment or cut surface, versus PGA on the ground surface as illustrated in Fig. 10.8. A relationship was established by linear regression analysis relating PGD to PGA on the ground surface in the free field. The median threshold value of PGA was then obtained for each damage state based on the aforementioned relationship and the definitions given in Table 10.2. The lognormal standard deviation, β_{tot} , which describes the total variability associated with each fragility curve, was estimated as described in Sect. 10.5.1. The estimated parameters of the fragility curves are presented in Tables 10.12 and 10.13. The derived curves are plotted in Figs. 10.16, 10.17, 10.18, and 10.19 for roadway and railway elements. For simplicity and in order to avoid intersection of the different fragility curves in case of the embankments, the plots are given for an average lognormal standard deviation equal to 0.9 for ground type C and 0.8 for ground type D.

Table 10.12 Parameters of numerical fragility curves for roadway and railway embankments in different ground types

Typology	Damage state	Ground type C				Ground type D			
		h = 2 m		h = 4 m		h = 2 m		h = 4 m	
		μ (g)	β	μ (g)	β	μ (g)	β	μ (g)	β
Roadway	Minor	0.65	1.00	0.51	0.90	0.47	0.90	0.31	0.70
	Moderate	1.04	1.00	0.88	0.90	0.66	0.90	0.48	0.70
	Extensive/ complete	1.57	1.00	1.42	0.90	0.89	0.90	0.72	0.70
Railway	Minor	0.52	1.00	0.36	0.90	0.40	0.90	0.25	0.70
	Moderate	0.77	1.00	0.57	0.90	0.53	0.90	0.37	0.70
	Extensive/ complete	1.17	1.00	0.91	0.90	0.72	0.90	0.54	0.70

Table 10.13 Parameters of numerical fragility curves for roadway and railway cuts in different ground types

Typology	Damage state	Ground type C		Ground type D			
		h = 6 m		h = 4 m		h = 6 m	
		μ (g)	β	μ (g)	β	μ (g)	β
Roadway	Minor	0.59	1.00	0.44	1.00	0.38	1.00
	Moderate	1.09	1.00	0.92	1.00	0.77	1.00
	Extensive/complete	1.90	1.00	1.77	1.00	1.46	1.00
Railway	Minor	0.44	1.00	0.31	1.00	0.27	1.00
	Moderate	0.74	1.00	0.58	1.00	0.49	1.00
	Extensive/complete	1.29	1.00	1.11	1.00	0.93	1.00

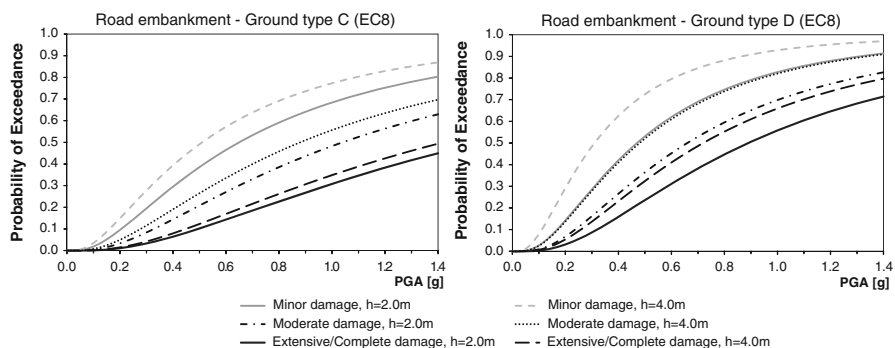


Fig. 10.16 Fragility curves for road embankments in ground type C (left) and D (right)

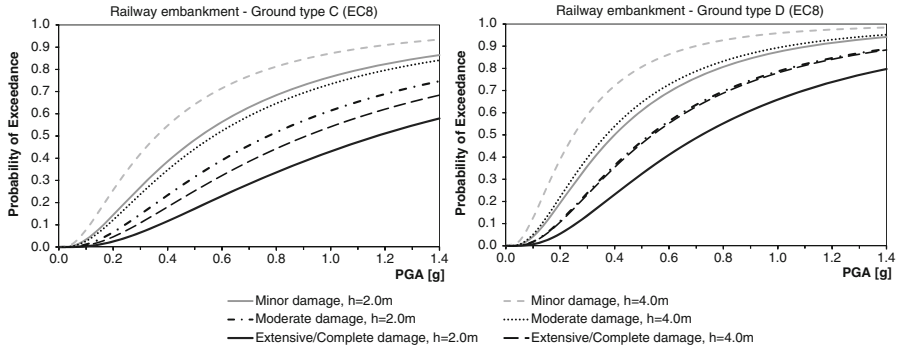


Fig. 10.17 Fragility curves for railway embankments in ground type C (left) and D (right)

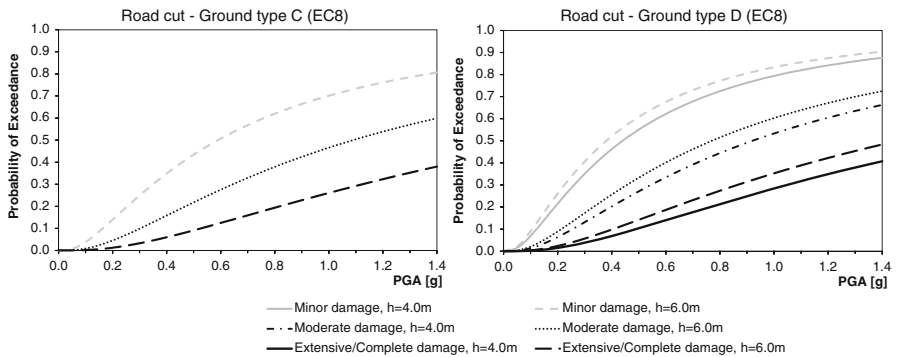


Fig. 10.18 Fragility curves for road cuts in ground type C (left) and D (right)

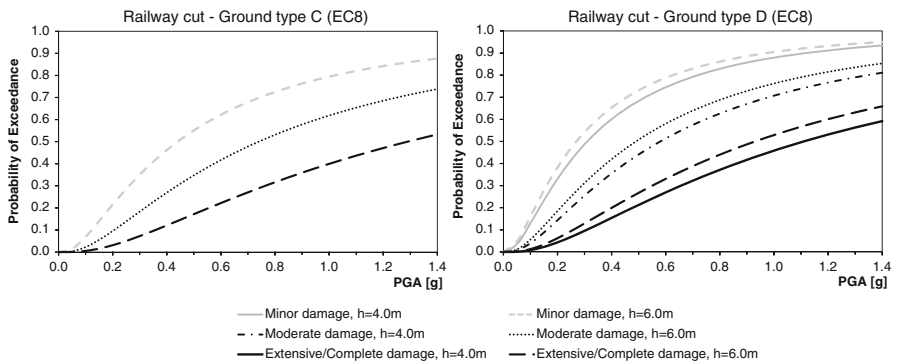


Fig. 10.19 Fragility curves for railway cuts in ground type C (left) and D (right)

10.6 Conclusions and Recommendations

A brief review of available fragility curves and their evaluation methods were presented for roadway and railway elements. The main typological features and damage states definitions were summarized. Tunnels, embankments, road pavements, slopes, cuts, railway tracks and bridge abutments are earth structures and are thus directly affected by the local soil conditions. In the framework of SYNER-G new analytical fragility curves are proposed for urban tunnels in alluvial soil, embankments and cuts, and bridge abutments for roadways and railways subjected to ground shaking. The effects of soil type and ground motion characteristics were taken into account by using typical soil profiles and seismic input motions. The response of the soil profiles was calculated through 1D equivalent linear analyses, while the non-linear response of the soil-structure system was calculated through 2D quasi-static or dynamic analyses. The available fragility curves for ground failure are limited; therefore, the case of the vulnerability of roadway and railway components due to liquefaction, landslide, rock-falls and fault rupture should further be investigated.

The proposed fragility functions for roadway and railway elements based on past and new developments presented herein are outlined in Table 10.14. Fragility functions for tunnels, embankments, cuts, slopes and bridge abutments correspond to ground shaking intensity in terms of PGA on the surface, while those for road

Table 10.14 Summary of proposed fragility functions for road/rail elements under ground shaking and ground failure

Element	Methodology	Classification	IMT
Urban tunnels in alluvial	SYNER-G Numerical analysis	Ground type: B, C, D (EC8) Circular (bored) Rectangular (cut and cover)	PGA
Other tunnels	ALA (2001) Empirical	Rock or alluvial/cut and cover Good or poor to average construction and conditions	PGA
Embankment (road/track on)	SYNER-G Numerical analysis	Ground type: C, D (EC8) Height: 2.0, 4.0 m	PGA
Cuts (road/track in)	SYNER-G Numerical analysis	Ground type: C, D (EC8) Height: 2.0, 4.0 m	PGA
Slopes (road/track on or running along)	SAFELAND (Pitilakis et al. 2010) Expert judgment/ empirical	Yield coefficient, k_y Earthquake magnitude	PGA
Bridge abutments	SYNER-G Numerical analysis	Ground type: C, D (EC8) Height: 6.0, 7.5 m	PGA
Road pavements (ground failure)	HAZUS Expert judgment	2 traffic lanes (Urban roads) >=4 traffic lanes (Major roads)	PGD
Railway tracks (ground failure)	SYNER-G Expert judgment	All	PGD

Table 10.15 General proposal for functionality of roadway elements

Damage state	Bridge	Tunnel	Embankment	Cut	Abutment	Slope	Road pavement
Minor	o	o	o	o	o	o	o
Moderate	p/o	c	p/o	p/o	p/o	p/o	p/o
Extensive/complete	c	c	c	c	c	c	

o open, *p/o* partially open (not applied when the roadway has one traffic lane), *c* closed

Table 10.16 Definition of functionality of roadway elements in relation to open traffic lanes before and after the earthquake

Damage state	Number of lanes each way open to traffic after EQ			
	Pre-EQ lanes = 1	Pre-EQ lanes = 2	Pre-EQ lanes = 3	Pre-EQ lanes = 4
Minor	1	2	3	4
Moderate	0	1	2	3
Extensive/complete	0	0	0	1

Table 10.17 General proposal for functionality of railway elements

Damage State	Bridge	Tunnel	Embankment	Cut	Abutment	Slope	Tracks
Minor	sr	sr	sr	sr	sr	sr	sr
Moderate	c	c	c	c	c	c	c
Extensive/complete	c	c	c	c	c	c	c

sr speed restriction, *c* closed

pavements and railway tracks are referred to ground failure in terms of permanent ground displacements.

The performance of a roadway system, at the component level, can be described through the reduction of functional traffic lanes due to damage, which is directly connected to the reduction of speed and capacity of the system. The general scheme in Table 10.15 can be used as a basis to estimate the functionality of roadway components due to different damage levels. Three levels of functionality are described, namely, open, partially open, and closed. The partially open state is defined based on the number of lanes of the undamaged road (Table 10.16), which is based on the REDARS approach (Werner et al. 2006). It is noted that the partially open state is not applied when the roadway has a single traffic lane. A general scheme for the functionality of railway elements is given in Table 10.17 where three levels of functionality are described (fully functional, functional but with speed restrictions, not functional/closed).

Acknowledgments The research leading to these results received funding from the European Community's 7th Framework Programme (FP7/2007-2013) under grant agreement n° 244061

References

- American Lifelines Alliance (ALA) (2001) Seismic fragility formulations for water systems, Part 1– Guideline, ASCE-FEMA, Reston, VA2001, 104 p
- Argyroudis S, Kaynia AM (2013) Analytical fragility functions for roadways and railways on embankments and in cuts due to seismic shaking, submitted to Bulletin of Earthquake Engineering
- Argyroudis S, Pitilakis K (2007) Development of vulnerability curves for circular shallow tunnels due to ground shaking and ground failure. In: Crosta GB, Frattini P (eds) Landslides: from mapping to loss and risk estimation. LESSLOSS report no. 2007/01. IUSS Press, Pavia, ISBN: 978-88-6198-005-1:175–184
- Argyroudis S, Pitilakis K (2012) Seismic fragility curves of shallow tunnels in alluvial deposits. *Soil Dyn Earthq Eng* 35:1–12
- Argyroudis S, Mitoulis S, Pitilakis K (2013a) Seismic response of bridge abutments on surface foundation subjected to collision forces. In: Proceedings of 4th international conference on computational methods in structural dynamics and earthquake engineering (COMPDYN), Kos Island, Greece, 12–14 June 2013
- Argyroudis S, Kaynia AM, Pitilakis K (2013b) Development of fragility functions for geotechnical constructions: application to cantilever retaining walls. *Soil Dyn Earthq Eng* 50:106–116
- ATC-13 (1985) Earthquake damage evaluation data for California. Applied Technology Council, Redwood City
- Bardet JP, Ichii K, Lin CH (2000) EERA: a computer program for equivalent-linear earthquake site response analyses of layered soil deposits. University of Southern California, Department of Civil Engineering, Los Angeles, 40 p
- Bray J, Travasarou T (2007) Simplified procedure for estimating earthquake-induced deviatoric slope displacements. *J Geotech Geoenviron Eng* 133(4):381–392
- Byers W (2004) Railroad lifeline damage in earthquakes. In: Proceedings of 13th world conference on earthquake engineering, Vancouver, BC, Canada, 1–6 Aug 2004, Paper No. 324
- Corigliano M (2007) Seismic response of deep tunnels in near-fault conditions. Ph.D. dissertation, Politecnico di Torino, Italy, p 222
- Dowding CH, Rozen A (1978) Damage to rock tunnels from earthquake shaking. *J Geotech Eng Div* 104:175–191
- EC8. Eurocode 8 (2004) Design of structures for earthquake resistance. European Committee for Standardisation, Brussels. The European Standard EN 1998-1
- Kaynia AM (ed) (2013) Guidelines for deriving seismic fragility functions of elements at risk: buildings, lifelines, transportation networks and critical facilities. SYNER-G reference report 4, Publications Office of the European Union, ISBN 978-92-79-28966-8, doi:[10.2788/19605](https://doi.org/10.2788/19605)
- Kaynia AM, Johansson J, Argyroudis S, Pitilakis K (2011) D3.8-Fragility functions for roadway system elements, Deliverable of SYNER-G EC Project
- Lagaros N, Tsompanakis Y, Psarropoulos P, Georgopoulos E (2009) Computationally efficient seismic fragility analysis of geostructures. *Comput Struct* 87:1195–1203
- LessLoss (2007) Risk mitigation for earthquakes and landslides, Research Project, European Commission, GOCE-CT-2003-505448
- Maruyama Y, Yamazaki F, Mizuno K, Tsuchiya Y, Yogai H (2010) Fragility curves for expressway embankments based on damage datasets after recent earthquakes in Japan. *Soil Dyn Earthq Eng* 30:1158–1167
- National Institute of Building Sciences (NIBS) (2004) HAZUS-MH: users’s manual and technical manuals. Report prepared for the Federal Emergency Management Agency, Washington, DC
- Owen GN, Scholl RE (1981) Earthquake engineering of large underground structures, in report no. FHWA/RD-80/195, Federal Highway Administration and National Science Foundation, 279 p

- Pitilakis K et al (2010) Physical vulnerability of elements at risk to landslides: methodology for evaluation, fragility curves and damage states for buildings and lifelines. Deliverable 2.5 in EU FP7 research project no. 226479. SafeLand: living with landslide risk in Europe: assessment, effects of global change, and risk management strategies
- Plaxis 2D (1998) Reference manual, version 7
- Plaxis 2D (2011) Reference manual, version 9
- Salmon M, Wang J, Jones D, Wu Ch (2003) Fragility formulations for the BART system. In: Proceedings of the 6th U.S. conference on lifeline earthquake engineering, TCLEE, Long Beach, 10–13 Aug 2003
- Werner SD, Taylor CE, Cho S, Lavoie J-P, Huyck C, Eitzel C, Chung H, Eguchi RT (2006) REDARS 2: methodology and software for seismic risk analysis of highway systems, MCEER-06-SP08
- Winter M, Smith JT, Fotopoulou S, Pitilakis K, Mavrouli O, Corominas J, Argyroudis S (2013) The physical vulnerability of roads to debris flow. In: Proceedings of the 18th international conference on soil mechanics and geotechnical engineering, Paris, 2–6 Sept 2013